Exergy analysis of a ground-source heat pump coupled with a phase change material energy storage system

Jesús Marcos García-Alonso[a], Natalia Muñoz-Rujas[b], Fernando Aguilar[c] and Eduardo Montero[d]

[a] University of Burgos, Burgos, Spain, jmgalonso@ubu.es
[b] University of Burgos, Burgos, Spain, nmrujas@ubu.es
[c] University of Burgos, Burgos, Spain, faguilar@ubu.es
[d] University of Burgos, Burgos, Spain, emontero@ubu.es

Abstract:

Latent heat thermal energy storage is particularly attractive technique because it provides a high energy storage density. There exist several studies on the energy and exergy analysis of coupled renewable energy and phase change materials (PCM) systems for the space heating and hot water production, most of them related to solar systems. But, as a renewable energy technology, ground source heat pump (GSHP) system should be considered as high efficient for space heating and cooling in buildings. GSHP application is growing rapidly as it is integrated with PCM system. Nevertheless, exergy analysis of these systems is still scarce. The paper presents an exergy analysis of a coupled GSHP+PCM system. For this purpose, an experimental bench has been developed to test the energy and exergy behaviour of such a system. The storage temperature and the size of the PCM container has been chosen to meet the energy needs for the heating and the domestic hot water supply of a single family house of about 150 m^2. A GSHP supply the energy needed to charge/discharge the PCM energy storage. Results of the energy and exergy analysis during the charging and discharging modes are presented.

Keywords:

Ground-source heat pump, latent energy storage, exergy.

1. Introduction

Thermal energy storage (TES) is a promising technology that is being promoted because it can reduce the energy consumption thereby limiting the environmental impact of energy. TES, which is also one of the key technologies for energy conservation, can be defined as temporary storage of thermal energy at low or high temperatures. It is best suited for heating and cooling thermal applications, because it provides a high energy storage density. TES can be carried out by means of sensible or latent heat energy storage. When compared to a conventional sensible heat energy storage system, latent heat energy storage system requires a smaller weight and volume of material for a given amount of energy. In addition, latent heat storage has the capacity to store heat of fusion at a constant or near constant temperature which corresponds to the phase transition temperature of the phase change material (PCM) [1, 2].

Exergy analysis is treated as a key tool to provide an alternative means of assessing and comparing TES systems. It is possible to define thermodynamic inefficiencies and loses using the exergy approach. So, exergy analysis can be used in improving and optimizing several of types TES designs. The studies on TES systems conducted up to date are widely based on the energetic analysis and assessments. In the scope of the exergy analysis of TES systems, the number of the studies on exergy analysis [i.e., 3-5] seems to be relatively scarce in the open literature. In a recent review, Verma et al. [6] have stressed the need for exergy analysis for TES units. There exist several studies on the energy and exergy analysis of coupled renewable energy and PCM systems for the space heating and hot

water production, most of them related to solar systems [7, 8]. But, as a renewable energy technology, ground source heat pump (GSHP) system should be considered as high efficient for space heating and cooling in buildings. GSHP application is growing rapidly as it is integrated with PCM system [9]. Nevertheless, exergy analysis of these systems is still scarce.

The paper presents an exergy analysis of a coupled GSHP+PCM system. For this purpose, an experimental bench has been developed to test the energy and exergy behaviour of such a system. The storage temperature and the size of the PCM container has been chosen to meet the energy needs for the heating and the domestic hot water supply of a single family house of about 150 m^2. A GSHP supply the energy needed to charge/discharge the PCM energy storage. Results of the energy and exergy analysis during the charging and discharging modes are presented.

2. System description

To test the heat transfer mode of a horizontal cylindrical shell and tube container for PCM energy storage, an experimental bench has been designed and built, as shown in Fig. 1. The PCM used is a hydrated salt with a melting temperature of 41ºC. It was selected because it is an adequate temperature for domestic hot water production and radiant floor heating. Table 1 presents the thermo-physical properties of the PCM, obtained from reference [10].

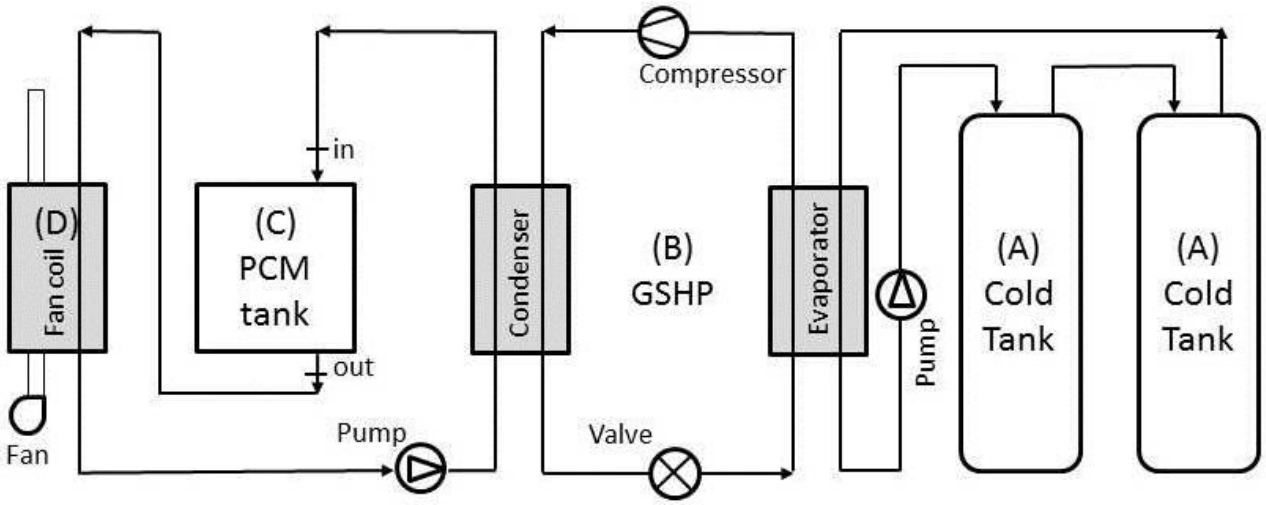

Fig. 1. Diagram of the experimental bench for testing the heat transfer rate of PCM placed in a cylindrical shell and tube container.

The storage temperature and the size of the container has been chosen to meet the energy needs for the heating and the domestic hot water supplies of a single family house of about 150 m^2. A Ground-Source Heat Pump (GSHP) supply the energy needed to charge/discharge the PCM energy storage.

Table 1. Thermo-physical properties of the PCM placed inside the cylindrical container [10].

Phase Change Temperature (ºC)		Latent Heat Capacity (kJ/kg)		Density (kg/m^3)
41		210		1587
Specific Heat Capacity (kJ/kg·K)			Thermal Conductivity (W/m·K)	
Solid	Liquid		Solid	Liquid
1,68	2,59		0.450	0.245

The experimental bench consists of (A) two water tanks, from Domusa™, model SANIT 150, each one of 150 l of volume, equipped with temperature control to set the temperature of the cold-source of the heat pump between 10ºC and 40ºC; (B) the GSHP from Giordano™, model SUNEO N5 (open loop heat pump, which uses the two tanks A as if they were aquifer energy sources), nominal heating power 5.35 kW, fluid R-407C; (C) one horizontal storage tank of 210 l, filled with the PCM modules; (D) one fan-coil Saunier Duval™, model 3-020 AF, to dissipate the energy stored in the PCM water tank, simulating the energy use in a single family house. For energy calculation purposes, the experimental stand was equipped with two thermal energy meters Kundo™, model G20/G21, class B, which includes two temperature probes Pt1000 and a flow meter with a maximum relative error of ±4%. Every energy meter corresponds with the measurements of the mass flow, inlet and outlet temperatures of the HTF with the GSHP and the fan-coil. All the measurement devices are computer controlled by means of the Agilent VEE 7.0 software.

The PCM is encapsulated in cylindrical tubes, each of 1000 mm long and 50 mm external diameter, 2 mm thickness. The tubes are made of high density polyethylene, with a thermal conductivity of 0.2 W/m·K. The stainless steel cylindrical tank is 1020 mm long and 510 mm internal diameter, with a capacity of 210 l. It is placed in horizontal position, with 1 inch diameter of input and output nozzles. The tank is externally insulated with a blanket of thickness 50 mm made of a commercial elastomer whose thermal conductivity is 0.04 W/m·K. Five baffles are placed inside the container, to stand the PCM tubes in horizontal position, then the container could be considered as a shell and tube heat exchanger. A maximum of 24 PCM tubes can be allocated inside the container. The holes of the baffles are made of higher diameter than those of the PCM tubes, in order to allow the water-flow. Figure 2 shows the geometrical distribution of PCM tubes.

Fig. 2. Configuration of PCM tubes and baffles inside the circular section of the container.

A set of 10 Pt100 temperature probes have been used to obtain the temperature distribution inside the shell and tube tank, as shown in Fig. 3. T103 to T107 probes measure the outside temperature of the tank, T102 measures the inner water temperature, T115 and T116 register the temperature of the internal surface of the PCM tubes and T117 and T118 measure the temperature of the external surface of the same. Ambient temperature, and inlet and outlet temperatures of water are also measured.

Temperature measurement was performed by means of the Pt100 probes and the multi-meter Agilent 34970A. After calibration of the equipment, uncertainty of temperature measurement has been estimated to be less than 0.05 K.

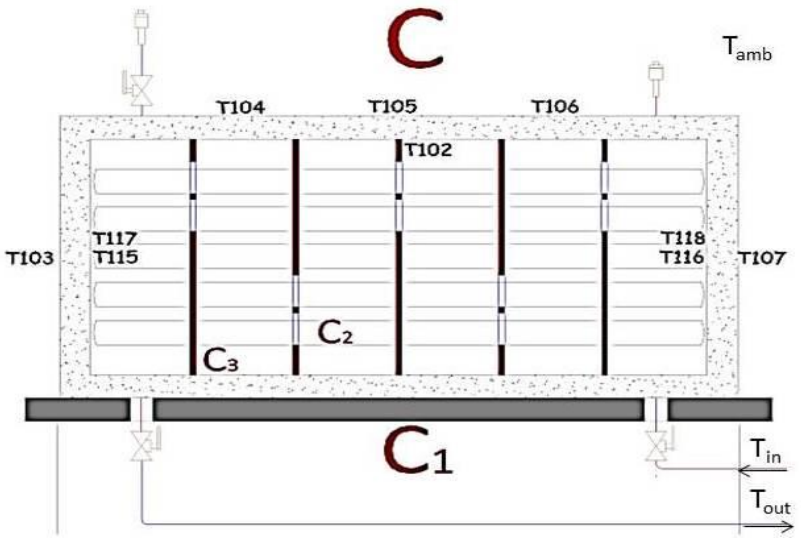

Fig. 3. Distribution of Pt100 temperature probes in the shell and tube cylindrical container C. PCMs are placed inside the tubes (C2) while water flows by the external surface (C3).

Figure 4 shows a typical energy charging/discharging mode of the PCM storage tank on a daily basis. The conditions during the experiment are that GSHP operates 14 h (from 22.00h to 12.00h, when the electricity cost is cheaper) while the fan-coil operates 24.00h (all day house demand). The hot water as HTF is supplied by the GSHP, and the set point is fixed at 50ºC. During the charging period, the GSHP starts heating the HTF, and the PCM in solid phase increases its temperature during the sensible heat transfer stage, before melting, showing a quasi-linear slope in the increasing temperature. When the melting temperature of PCM is reached (41ºC) at the external surface of the PCM, it starts changing to the latent heat transfer mode and melting process takes place. The rate of temperature increase is smaller, and the slope of the curve then decreases compared to the sensible mode. Along this period, heat from the HTF is transferred to the PCM through the thermal resistance of the polyethylene tube by heat conduction.

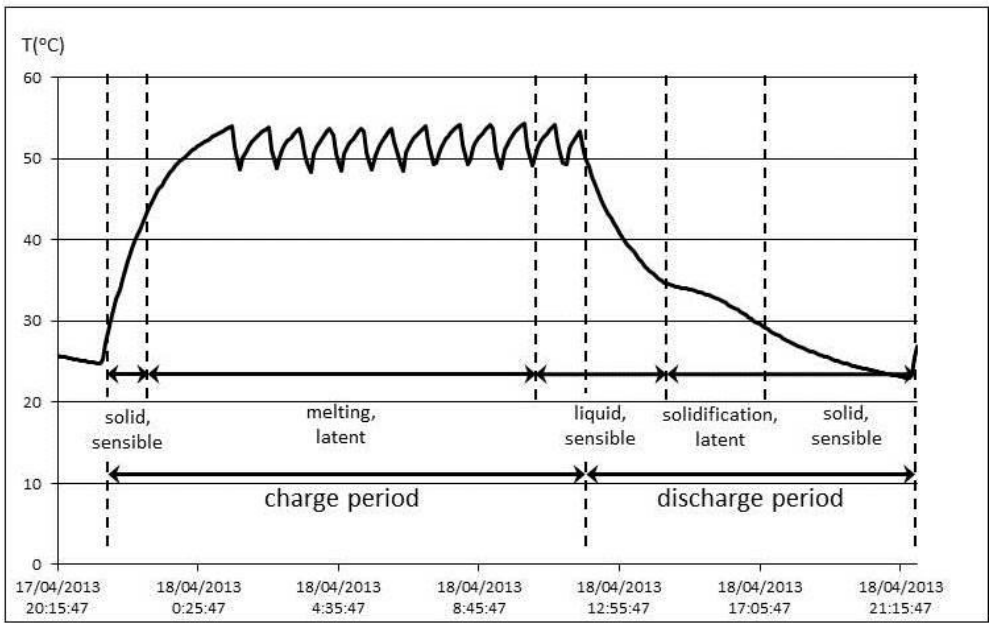

Fig. 4. Distribution of the HTF temperature vs. time along the charge and discharge periods of the PCM container

Once the set-point of 50ºC is reached by the HTF, typical temperature evolution of the temperature in a saw-tooth shape around the temperature set point occurs, as the GSHP is on/off controlled. This mode is kept repeatedly along the rest of the charging period. Along this period, the PCM ends its melting and all the PCM is in the liquid phase. Moreover, superheating of the liquid PCM should take place if the GSHP still continues working. It should be noticed that, at a fixed time, the radius of the moving boundary of the melting PCM will be different along the axial direction of the tube, and also the temperature of the liquid phase in contact with the local temperature of the HTF.

When the GSHP ends its heat supply, only the fan-coil is in operation, and the discharging period starts, the PCM being in the liquid phase. Initially, the PCM temperature decreases as sensible heat exchanges, and super-cooling of the PCM (under its nominal solidification temperature) could sometimes appear. When solidification of the PCM begins, the temperature profile shows a nearly flat shape, enlarging the period of time of energy availability at a useful temperature, which constitutes one of the advantages of the PCM. After the solidification ends, then the discharge uses the sensible heat exchange of the solid PCM.

3. Exergy analysis

In general, exergy analysis is based on the thermodynamic concepts associated with second law of thermodynamics along with conservations principles of mass and energy. It is widely proved that exergy analysis is a very effective tool or compliment to energy analysis for performance assessment and optimization of thermal systems. This section presents the exergy method of the device described in section 2. Exergetic performance of the system is experimentally investigated during both charging and discharging periods.

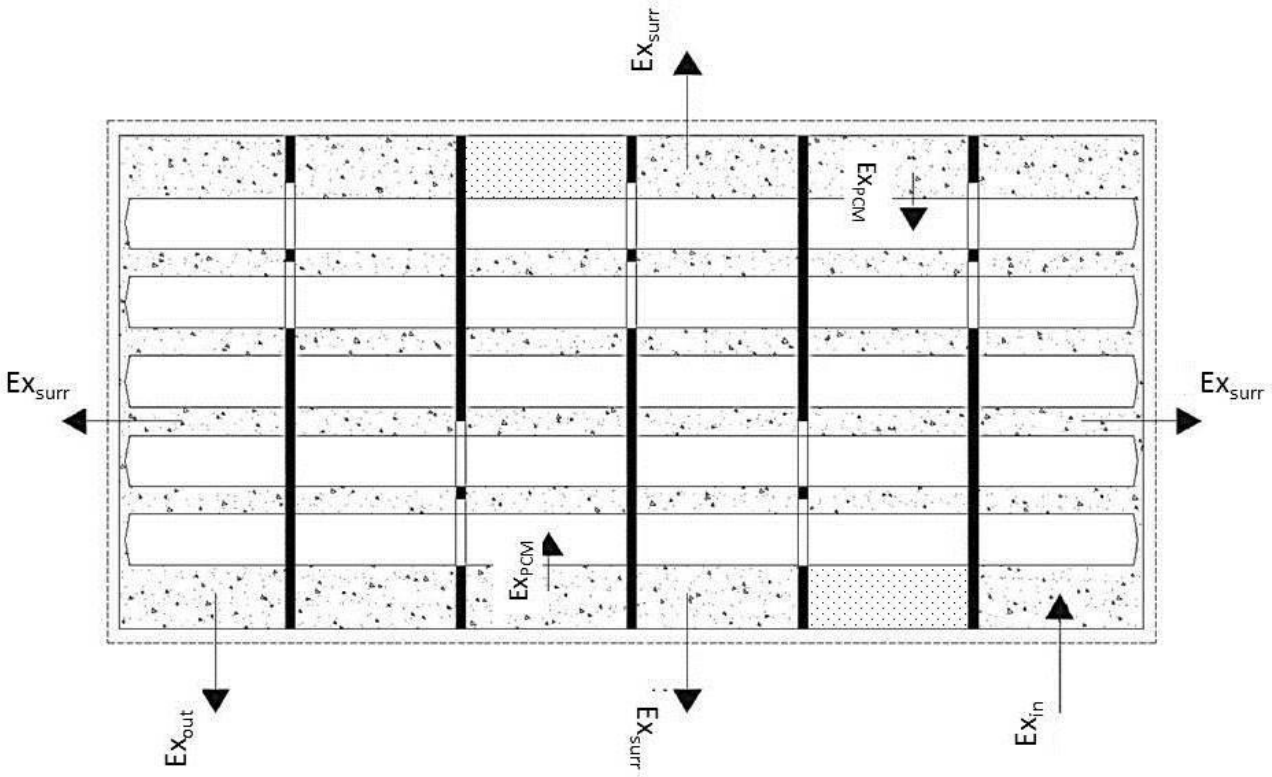

Fig. 5. Distribution of exergy exchanges in the shell and tube cylindrical container. The control volume is the heat transfer fluid HTF

The evaluation of exergy efficiency for the system requires evaluation of exergy associated with the exergy exchanges of the selected control volume, which is the portion of HTF inside the cylindrical

container, following Fig. 5. Exergy input comes from the inlet fluid, Ex_{in}, while exergy exits refers to the exergy output to the outlet fluid, Ex_{out}, and the to the exergy due to the heat transfer with the surroundings, Ex_{surr}, at the ambient temperature reference, T_0. Exergy exchange with the PCM, Ex_{PCM}, also occurs, as well as some exergy destruction due to the internal irreversibilities, $Ex_{destroyed}$. The, the exergy stored by the HTF within the control volume, Ex_{stored}, can be expressed by means of the exergy balance

Exergy input – (Exergy output + Exergy destroyed) = Exergy stored

or, since the heat transfer is time dependent, when considering the exergy by time unit, $\dot{E}x$

$$\dot{E}x_{in} - \left(\dot{E}x_{out} + \dot{E}x_{surr} + \dot{E}x_{PCM} + \dot{E}x_{destroyed}\right) = {}^{dEx_{stored}}/_{dt} \qquad (1)$$

The exergy of the respective inlet and outlet fluid in relation with the control volume could be expressed, as

$$\dot{E}x_{in} = \dot{m}_{HTF}\left[\left(h_{HTF,in} - h_{HTF,0}\right) - T_0(s_{HTF,in} - s_{HTF,0})\right] \qquad (2)$$

$$\dot{E}x_{out} = \dot{m}_{HTF}\left[\left(h_{HTF,out} - h_{HTF,0}\right) - T_0(s_{HTF,out} - s_{HTF,0})\right] \qquad (3)$$

being $\dot{m}_{HTF}$, $h_{HTF,in}$, $h_{HTF,out}$, $s_{HTF,in}$ and $s_{HTF,out}$, the mass flow, the inlet and the outlet enthalpy, and the inlet and the outlet entropy of the heat transfer fluid at their respective p, T conditions. In the same manner, $h_{HTF,0}$ and $s_{HTF,0}$ represent the enthalpy and entropy of the heat transfer fluid in equilibrium with ambient conditions p_0, T_0. All the properties needed to estimate the exergy input and output of (2) and (3) are obtained from the respective energy meters and temperature probes described in Section 2.

Concerning the exergy exchanged with the surroundings, $\dot{E}x_{surr}$, due to the heat transfer between the HTF temperature (probe T102) and the ambient temperature T_0, Q_{surr}, the exergy estimation leads to

$$\dot{E}x_{surr} = Q_{surr}\left(1 - \frac{T_0}{T_{102}}\right) \qquad (4)$$

The heat transfer, Q_{surr}, has been estimated taking into account the external surface of the cylindrical and plate walls, the width of the insulation blanket and the inside (probe T102) and outside temperature walls (probes T103 to T107).

With respect to the exergy exchange with the PCM, $\dot{E}x_{PCM}$, we have to point out that, as the control volume is the HTF inside the tank, the exergy exchange between the HTF and the PCM should be computed considering only the exergy transfer from the HTF inside the control volume, at tempertaure T_{102}. Then we used the expression

$$\dot{E}x_{PCM} = Q_{PCM}\left(1 - \frac{T_0}{T_{102}}\right) \qquad (5)$$

where the heat exchange with the PCM, Q_{PCM}, is estimated considering the conduction heat transfer between the PCM and the HTF through the cyclindrical surface of the encapsulated PCM and its measured internal and external temperatures (probes T115 to T118). During the charging period, $T_{102} > T_{PCM}$, and Q_{PCM} will exit the HTF, while when the discharging period occurs, $T_{102} < T_{PCM}$ and Q_{PCM} will enter the HTF.

Finally, the stored exergy by the HTF, Ex_{stored}, could be expressed as

$$Ex_{stored} = m_{tank}[(h_{102} - h_0) - T_0(s_{102} - s_0)] \quad (6)$$

where m_{tank}, h_{102} and s_{102} are the mass of HTF inside the tank, the enthalpy and the entropy of the HTF at the temperature T_{102} of the HTF inside the control volume, respectively.

Though charging and discharging exergy efficiencies could be defined [11, 12], in this work we consider most convenient to use an overall exergy efficiency [7]. The operation of thermal energy storage systems is inherently a cycle comprised of energy storage process followed by energy removal process. Hence, the calculation of overall cycle exergy efficiency becomes necessary. We point out that the concept of cycle refers to the 24h time operation of the device and not to a thermodynamic cycle where all the state properties comes back to the initial values. Moreover, depending on the power output of the fan-coil, the temperature and any related property of the HTF inside the control volume could show a finite variation from the initial to the final state along the 24h cycle.

Then, the overall exergy efficiency is defined as

$$\phi_{ex} = \frac{Exergy\ HTF,out + Exergy\ stored\ by\ HTF,final\ state}{Exergy\ HTF,in + Exergy\ stored\ by\ HTF,initial\ state} \quad (7)$$

which is a definition from the user point of view. This definition concerns the efficiency as a ratio amongst the total available exergy from the storage tank and the exergy contents in the tank due to the exergy storage and the exergy supply. Hence, there is not a maximum exergy storage capacity of TES that can serve as reference, but a relative efficiency that concers the user interest.

4. Results and discussion.

As stated in section 2, the conditions during the experiment are that GSHP operates 14 h, from 22.00h to 12.00h, while the fan-coil operates 24.00h. Data are recorded every 300 seconds, the full cycle of 24h gives N = 288 sets of data. From N = 0 (initial state, t = 0) to N = 168 the charging period takes place, while from N = 168 to N = 288 the discharging period occurs. Then, the overall exergy efficiency (7) can be expressed as

$$\phi_{ex} = \frac{\sum_{j=1}^{288} Ex_{out} + Ex_{stored(288)}}{\sum_{j=1}^{288} Ex_{in} + Ex_{stored(0)}} \quad (8)$$

Three experiments were carried out to test the exergy performance of the test bench. The power of the fan-coil could be fixed at three speeds of the fan, which led to three volumetric air-flows: 160, 250 and 390 m^3/h, respectively, which will be named cases A, B and C.

Figures 6, 7 and 8 show the integrated values, over the period of 24h, of the exergy exchanges and storage concerning (1).

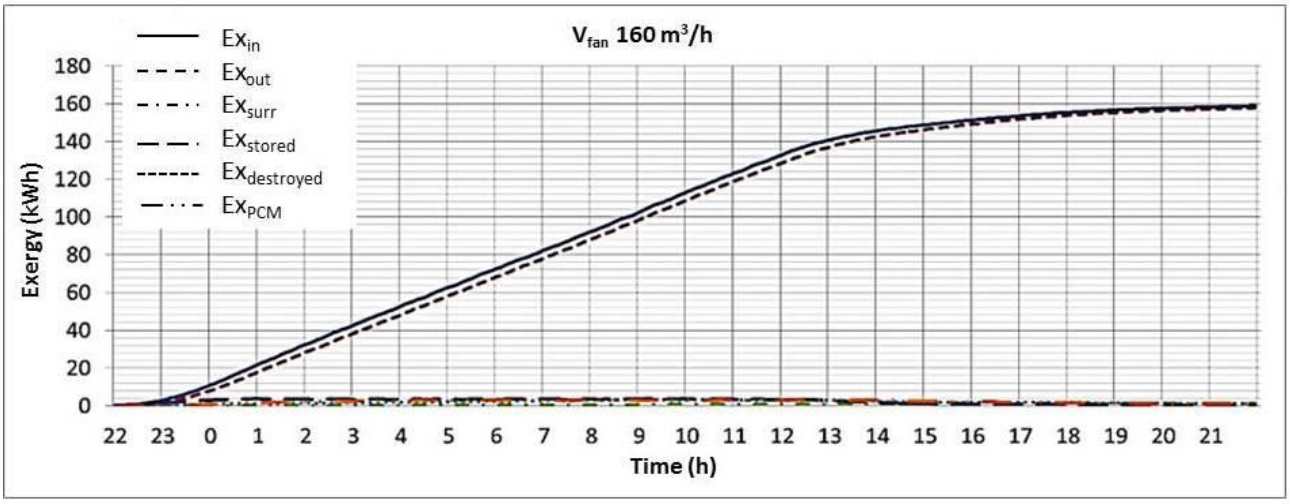

Fig. 6. Integrated exergy values versus time for the experimental set-up. Test A, volumetric flow of the fan-coil 160 m³/h.

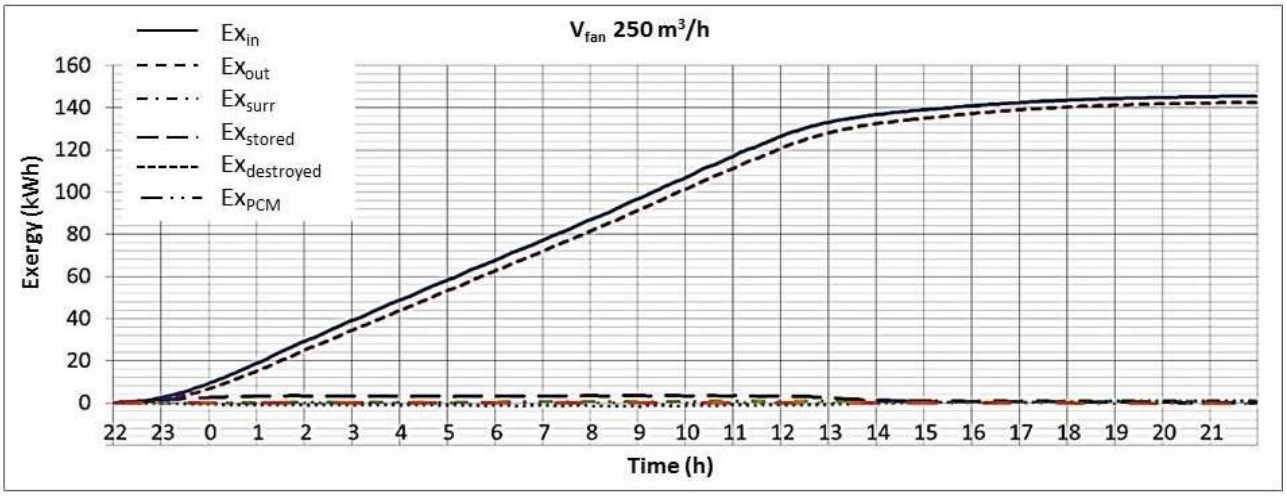

Fig. 7. Integrated exergy values versus time for the experimental set-up. Test B, volumetric flow of the fan-coil 250 m³/h.

From observation of Fig. 6 to 8 and Table 2, it can be seen that, as expected, the accumulated exergy input and output decreases as the energy demand of the user increases, it is to say, as the volumetric air-flow of the fan increases. The result is explained by the decrease of the heat transfer fluid through the whole system when the energy demand of the user increases. During the charging period, the exergy input and exergy output rates keep almost constant, which leads to the positive slope of the respective integrated exergy curves. While the discharging period (GSHP switched-off, fan-coil switched-on) the integrated exergy output shows no change, as the output temperature is kept almost constant by the energy supplied by the PCM. During the charging period, the difference between the exergy input and the exergy output is explained by the exergy stored by the HTF, which is still a very small amount in comparison with the exergy input.

Table 2. Exergy exchanges of the storage tank as defined in (8).

Case	Ex_{in} (kWh)	Ex_{PCM} (kWh)	Ex_{surr} (kWh)	Ex_{out} (kWh)	$Ex_{destroyed}$ (kWh)
A	158.78	1.07	1.09	157.75	1.23
B	145.47	0.89	1.00	142.59	0.98
C	133.36	0.61	0.96	131.49	0.29

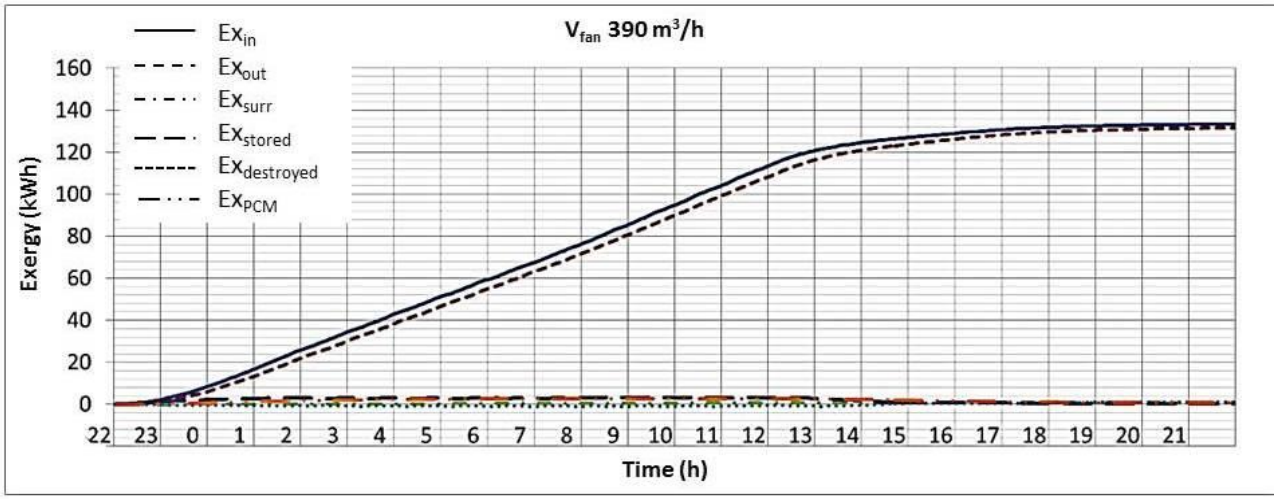

Fig. 8. Integrated exergy values versus time for the experimental set-up. Test C, volumetric flow of the fan-coil 390 m^3/h.

At the same time, the exergy exchanged with the surroundings keeps almost constant independently of the energy demand, presenting an average of 0.7% in relation to the exergy input. Almost the same concerns the destroyed exergy, which keeps in the range from 0.2% to 0.8% of the exergy input.

Table 3. Integrated exergy efficiencies of the storage tank as defined in (8).

Case	Fan volumetric flow (m^3/h)	Exergy efficiency, ϕ (%)
A	160	99.41
B	250	98.03
C	390	98.61

Table 3 shows that the exergy efficiency, as defined by (8) decreases more than linearly as the volumetric flow of air in the fan-coil increases. This variation could be due to the simultaneous change in the temperatures used to estimate the exergy content of the input and output of the heat transfer fluid by (2) and (3). It can be supposed that the exergy supply of the GSHP tends to follow the increase of the exergy demand of the fan-coil, because of the higher exergy extraction due to the higher value of the air-flow. Nevertheless, there seems to be a delay between the variation of temperatures of the HTF entering and leaving the tank, leading to a faster increase in the ratio of extraction of exergy with respect to the exergy supply.

5. Conclusions

A case study of exergy analysis of a low-temperature PCM energy storage system coupled with a ground source heat pump has been presented. An experimental bench has been developed to test the exergy behaviour of such a system. The study has shown data on the characterization of the exergy balance of a PCM stored in a horizontal cylindrical shell and tube heat exchanger, being the PCM placed inside the tubes. Three different cases were studied varying the ratio of exergy extracted from the PCM storage tank. Results show that exergy exchange with the surroundings and the destruction of exergy due to internal irreversibilities were kept almost constant. During the charging period, the exergy input and exergy output rates keep almost constant, while the integrated exergy output shows no change along the discharging period. The defined user's exergy efficiency, as a ratio amongst the total available exergy from the storage tank and the exergy contents in the tank due to the exergy storage and the exergy supply, tends to decrease as the exergy extracted increases.

Acknowledgments

We acknowledge support for this research to the company ENERFUTURE S.L.L., Spain, project on "Integration of low-temperature storage and renewable energy systems in air-conditioning of small scale buildings", ENERFUTURE-Universidad de Burgos, 2010.

This contribution is part of the Thesis Doctoral of J. M. García-Alonso

Nomenclature

c	specific heat capacity, kJ/kg·K
GSHP	ground source heat pump
Ex	exergy, kWh
$\dot{E}x$	exergy power, kW
fan	fan-coil
HTF	heat transfer fluid
$\dot{m}$	mass flow, kg/s
N	number of data points
PCM	phase change material
Q	heat transfer, kW
surr	surroundings
t	time, s
T	temperature, K
T_0	reference temperature, K
TES	thermal energy storage

Greek symbols

ϕ_{ex}	exergy efficiency

References

[1] Dinçer, I., Rosen, M. A., Thermal Energy Storage Systems and Applications, Wiley, London, 2011.

[2] Abhat, A. Low temperature latent heat thermal energy storage: heat storage materials. Solar Energy 1983;30:313–332.

[3] Rosen M.A., Tang R., Dincer I., Effect of stratification on energy and exergy capacities in thermal storage systems, International Journal of Energy Research 2004;28:177–193.

[4] Ramayya A.V., Ramesh K.N., Exergy analysis of latent heat storage systems with sensible heating and subcooling of PCM, International Journal of Energy Research 1998;22:411–426.

[5] Keshavarz A., Ghassemi M., Mostafavi A., Thermal energy storage module design using energy and exergy analysis, Heat Transfer Engineering 2003;24:76–85.

[6] Verma P, Varun, Singal SK., Review of mathematical modelling on latent heat thermal energy storage systems using phase-change material. Renew Sustain Energy Rev 2008;12:999–1031.

[7] Jegadheeswaran S., Pohekar S.D., Kousksou T., Exergy based performance evaluation of latent heat thermal storage system: A review, Renew Sustain Energy Rev 2010;14:2580–2595

[8] Fazilati M.A., Alemrajabi A.A., Phase change material for enhancing solar water heater, an experimental approach, Energy Conversion and Management 2013;71:138–145.

[9] Zhu N., Hu P., Xu L., Jiang Z., Lei F., Recent research and applications of ground source heat pump integrated with thermal energy storage systems: A review, Applied Thermal Engineering 2014;71:142-151.

[10] Plus Ice©, Phase Change Materials (PCM) Thermal Energy Storage (TES) Design Guide, Phase Change Material Products Ltd, Yaxley, Cambridgeshire, UK, 2011.

[11] Ezan M. A., Ozdogan M., Gunerhan H., Erek A., Hepbasli A., Energetic and exergetic analysis and assessment of a thermal energy storage (TES) unit for building applications, Energy and Buildings 2010;42:1896–1901.

[12] Öztürk H.H., Experimental evaluation of energy and exergy efficiency of a seasonal latent heat storage system for greenhouse heating, Energy Conversion and Management 2005;46:1523–1542.